

Universitat de Lleida

Document downloaded from:

<http://hdl.handle.net/10459.1/69877>

The final publication is available at:

<https://doi.org/10.1111/gcb.14038>

Copyright

(c) John Wiley & Sons Ltd, 2018

1
2
3
4
5
6
7
8
9
10
11
12
13
14
15
16
17
18
19
20
21
22
23

DR. LUKE COLLINS (Orcid ID : 0000-0001-8059-0925)

DR. REMKO DUURSMA (Orcid ID : 0000-0002-8499-5580)

Article type : Primary Research Articles

Understorey productivity in temperate grassy woodland responds to soil water availability but not to elevated [CO₂]

Running head: Understorey productivity in elevated [CO₂]

Authors: Collins, L.^{1*}, Bradstock, R.A.², Resco de Dios, V.³, Duursma, R.A.¹, Velasco, S.², Boer, M.M.¹

¹ Hawkesbury Institute for the Environment, Western Sydney University, Locked Bag 1797, Penrith, Australia, 2751

² Centre for Environmental Risk Management of Bushfires, University of Wollongong, Wollongong, NSW, Australia, 2500

³ Department of Crop and Forest Sciences and Agrotecnio Center, Universitat de Lleida, Lleida, 25198, Spain

* Current address: Department of Ecology, Environment & Evolution, La Trobe University, Bundoora, Victoria, Australia, 3086; Arthur Rylah Institute for Environmental Research, Department of Environment, Land, Water and Planning, PO Box 137, Heidelberg, Victoria, Australia, 3084

This is the author manuscript accepted for publication and has undergone full peer review but has not been through the copyediting, typesetting, pagination and proofreading process, which may lead to differences between this version and the [Version of Record](#). Please cite this article as [doi: 10.1111/gcb.14038](https://doi.org/10.1111/gcb.14038)

24 **Corresponding author:** Luke Collins, tel +61 421 436 588, email:

25 lcollins241181@gmail.com

26 **Keywords:** drought, free air CO₂ enrichment, phenocam, phenology, stereo camera

27 **Paper type:** Primary Research

28 **Abstract**

29 Rising atmospheric [CO₂] and associated climate change are expected to modify primary
30 productivity across a range of ecosystems globally. Increasing aridity is predicted to reduce
31 grassland productivity, though rising [CO₂] and associated increases in plant water use
32 efficiency may partially offset the effect of drying on growth. Difficulties arise in predicting
33 the direction and magnitude of future changes in ecosystem productivity, due to limited field
34 experimentation investigating climate and CO₂ interactions. We use repeat near-surface
35 digital photography to quantify the effects of water availability and experimentally
36 manipulated elevated [CO₂] (eCO₂) on understorey live foliage cover and biomass over three
37 growing seasons in a temperate grassy woodland in south-eastern Australia. We hypothesised
38 that (i) understorey herbaceous productivity is dependent upon soil water availability, and (ii)
39 that eCO₂ will increase productivity, with greatest stimulation occurring under conditions of
40 low water availability. Soil volumetric water content (VWC) determined foliage cover and
41 growth rates over the length of the growing season (August - March), with low VWC (< 0.1
42 m³ m⁻³) reducing productivity. However, eCO₂ did not increase herbaceous cover and
43 biomass over the duration of the experiment, or mitigate the effects of low water availability
44 on understorey growth rates and cover. Our findings suggest that projected increases in
45 aridity in temperate woodlands are likely to lead to reduced understorey productivity, with
46 little scope for eCO₂ to offset these changes.

47 **Introduction**

48 Concentrations of atmospheric CO₂ have risen at unprecedented rates since the industrial
49 revolution, resulting in increased global temperatures and reduced precipitation across many
50 biomes (IPCC, 2014). Global climate change and elevated atmospheric [CO₂] (eCO₂) can
51 modify ecosystem primary productivity via changes to plant growth, mortality and
52 phenology, influencing carbon fluxes between the atmosphere and biosphere (Hufkens *et al.*,

53 2016, Ma *et al.*, 2015, Reyes-Fox *et al.*, 2014, Zhu *et al.*, 2016b). Modelling, satellite and
54 field studies have found evidence that eCO₂ can increase ecosystem productivity and carbon
55 sequestration across many terrestrial biomes (Donohue *et al.*, 2013, Kolby Smith *et al.*, 2016,
56 Morgan *et al.*, 2004), partially offsetting global emissions (Ballantyne *et al.*, 2012). Earth
57 system models used to set greenhouse gas emission targets have been shown to over-predict
58 the enhancement of productivity associated with increasing [CO₂], partially owing to poor
59 representation of climate feedbacks within temperate and arid ecosystems (Kolby Smith *et*
60 *al.*, 2016). Experimental research aimed at understanding the interactive effects of CO₂ and
61 climate on ecosystem productivity will be instrumental in facilitating improved predictions of
62 ecosystem change under future climates (Hufkens *et al.*, 2016, Kolby Smith *et al.*, 2016).

63 Increased atmospheric [CO₂] can stimulate plant growth and ecosystem productivity directly
64 by increasing rates of CO₂ assimilation in C3 species, and indirectly by reducing stomatal
65 conductance in C3 and C4 species, potentially resulting in greater soil water availability
66 (Ainsworth & Long, 2005, Morgan *et al.*, 2004). In periodically water limited ecosystems
67 (e.g. semi-arid and temperate grasslands), water savings are the primary mechanism through
68 which eCO₂ may increase ecosystem productivity and growing season length (Morgan *et al.*,
69 2004), though increased CO₂ assimilation may also be important (Pathare *et al.*, 2017). Field
70 based CO₂ enrichment studies have shown that eCO₂ typically increases productivity during
71 periods of rainfall deficit, with eCO₂-induced water savings increasing water availability and
72 consequently growth (Hovenden *et al.*, 2014, Morgan *et al.*, 2011, Morgan *et al.*, 2004).

73 Increased net primary productivity under eCO₂ may arise from both increased growth rates
74 and an extension of the growing season, by prolonging the final days of growth or reducing
75 the number of periodic drought days throughout the growing season (Morgan *et al.*, 2004).
76 Water savings may also enhance productivity under a warming climate by counteracting
77 increased evaporative demand (Morgan *et al.*, 2011), which may be particularly evident
78 during periods of low moisture availability.

79 Grass dominated ecosystems, including woodlands and savannas that consist of a mixture of
80 grasses and trees, occupy a large portion of the terrestrial biome (> 30%) and account for ~30
81 % of global aboveground net primary production (NPP) (Asner *et al.*, 2004, Del Grosso *et al.*,
82 2008). These ecosystems characteristically experience periods of water limitation, due to
83 highly seasonal rainfall (e.g. Mediterranean grasslands, tropical savannas) or unpredictable
84 wet/dry periods (e.g. temperate woodlands, semi-arid grasslands) (Lehmann *et al.*, 2011, Lunt

85 *et al.*, 2012, Morgan *et al.*, 2004). Ecosystem productivity, community composition and
86 grass-tree ratios are strongly mediated by water availability, though temperature, edaphic
87 factors and disturbances such as fire and herbivory also exert considerable influence (Del
88 Grosso *et al.*, 2008, Lehmann *et al.*, 2014, Lunt *et al.*, 2012, Sala *et al.*, 2012). Due to the
89 importance of water availability for grassland growth, grass productivity is likely to be highly
90 sensitive to increasing [CO₂] and climate change (e.g. Morgan *et al.*, 2011, Reyes-Fox *et al.*,
91 2014). Increasing atmospheric [CO₂] has been proposed as a major driver of recent
92 broadscale increases in ecosystem productivity, including grasslands (Kolby Smith *et al.*,
93 2016), and changes to grass-tree ratios in savannas (Bond & Midgley, 2012). Field
94 experimentation examining the sensitivity of grass productivity to eCO₂ and climatic patterns
95 is limited and has predominantly occurred in semi-arid and temperate grasslands (e.g.
96 Hovenden *et al.*, 2014, Morgan *et al.*, 2004, Reich *et al.*, 2014), with few studies taking place
97 in woodlands and savannas, where the response of the herbaceous understorey to eCO₂ may
98 have potentially far-reaching implications for ecosystem function and structure (e.g. through
99 effects on water balance, fuel properties and fire regimes; Bond & Midgley, 2012).

100 Studies examining the effect of eCO₂ and climate on grassland productivity have largely used
101 periodic (i.e. seasonal - annual) destructive harvesting, which only allows for the assessment
102 of aggregated climate effects on biomass production (e.g. Hovenden *et al.*, 2014, Reich *et al.*,
103 2014). However, grassland productivity is dynamic and responds to climatic events (e.g.
104 rainfall, drying, heatwaves) over short time frames (e.g. weeks) (Migliavacca *et al.*, 2011,
105 Morgan *et al.*, 2004, Pathare *et al.*, 2017). Consequently, high frequency measures of
106 ecosystem productivity are required to adequately capture climate and eCO₂ effects on
107 grassland productivity (Migliavacca *et al.*, 2011, Zelikova *et al.*, 2015), and will provide
108 greater value for the development and testing of process-based ecosystem models (Hufkens *et*
109 *al.*, 2016). Near-surface remote sensing using timelapse digital photography provides an ideal
110 tool for the quantification of trends in grassland growth at fine temporal scales (Hufkens *et*
111 *al.*, 2016, Migliavacca *et al.*, 2011, Zelikova *et al.*, 2015). Greenness indices derived from
112 digital photographs are highly correlated with grassland projected foliage cover and gross
113 primary productivity (Hufkens *et al.*, 2016, Migliavacca *et al.*, 2011, Moore *et al.*, 2016,
114 Toomey *et al.*, 2015, Zelikova *et al.*, 2015). Stereo imaging techniques are also effective at
115 characterising vegetation structure and can provide estimates of vegetation biomass (Yoon &
116 Thai, 2010).

117 We used near-surface digital photography and stereo imaging to measure and monitor the
118 response of understorey live foliage cover (3 day intervals) and aboveground biomass (~30 –
119 60 day intervals) to experimentally manipulated eCO₂, water availability and biotic factors in
120 a temperate grassy woodland over a ~2.5 year period comprising 3 full growing seasons. We
121 targeted the interactive effects of eCO₂ and water availability on understorey productivity, as
122 eCO₂ is predicted to mitigate the effect of increased aridity under future climate change
123 (Morgan *et al.*, 2011). We hypothesise that (i) understorey herbaceous productivity depends
124 on soil water availability, and (ii) there will be periodic increases in understorey productivity
125 under eCO₂, which will be greatest when soil moisture is limiting.

126 **Materials and Methods**

127 **Site description and study design**

128 The EucFACE Free Air CO₂ Enrichment experimental facility is located in a remnant
129 temperate Eucalypt woodland at Western Sydney University, Sydney, Australia (EucFACE;
130 33° 36' 58" S, 150° 44' 22.1" E). The tree canopy is dominated by *Eucalyptus tereticornis*
131 (~25 m tall) and is characterised by a relatively low foliage cover (low leaf area index 1.1 –
132 2.2 m² m⁻²) (Duursma *et al.*, 2016). The understorey is largely comprised of a mixture of C3
133 and C4 grasses and C3 forbs, with the native C3 grass *Microlaena stipoides* accounting for
134 ~70% of the herbaceous biomass (Pathare *et al.*, 2017). The C3 herbs *Commelina cyanea* and
135 *Pratia purpurascens*, the introduced C3 grass *Cynodon dactylon* and the C4 grass
136 *Cymbopogon refractus* are also common across the study site (Drake *et al.*, 2016). Shrub
137 cover is sparse and dominant species include *Melaleuca decora*, *Acacia parramattensis*,
138 *Breynia oblongifolia*, *Hakea sericea* and *Bursaria spinosa* (Drake *et al.*, 2016, Pathare *et al.*,
139 2017).

140 The EucFACE consists of six 25 m diameter circular plots (designated hereafter as ‘rings’)
141 each consisting of 32 vent pipes that extend above the tree canopy (~28 m tall). Prediluted
142 CO₂ is released through adjustable ports located at 50 cm intervals along the length of the
143 vent pipes and facing toward the centre of the ring. Three rings were randomly assigned to an
144 ambient CO₂ treatment and three assigned to the elevated treatment (ambient + 150 ppm
145 CO₂). The rings were constructed in 2010 and fumigation commenced in September 2012
146 (Drake *et al.*, 2016). The mean CO₂ concentrations at 20 cm above the ground for the three

147 eCO₂ rings over the first four years of fumigation (February 2013 – February 2017) ranged
148 between 565 ppm to 589 ppm, exceeding the target of ~550 ppm.

149 Four 2 m x 2 m understorey monitoring plots were randomly located in each ring prior to the
150 commencement of fumigation in September 2012. A Wingscapes timelapse camera (model
151 WTC-00122, Wingscapes, Alabaster, AL) was installed at each understorey plot in July 2014.
152 Cameras were attached to a horizontal crossbar extending from a vertical pole, so that they
153 were ~ 2.7 m above the ground and facing vertically downwards towards the centre of the
154 understorey plot (Fig. 1a). The support poles were located on the southern edge of the
155 understorey plot. The cameras used an automatic exposure and a fixed focus (2 m to ∞) and
156 photos were captured at the finest resolution possible (8 megapixels). Photos were captured at
157 10 minute intervals for at least one hour pre- and post-sunrise. Images captured shortly after
158 sunrise were targeted because they did not contain shadows from surrounding trees and site
159 infrastructure. Photos were captured between the 1st of August 2014 and the 31st of March
160 2017.

161 **Image greenness and live foliage cover**

162 Image analysis focused on a 1.5 m² (1.23 m x 1.23 m) region of interest at the centre of each
163 plot (Fig. 1b). The green chromatic coordinate index (GCC) was used in our study to quantify
164 the greenness of the live vegetation component, calculated using the following equation
165 (Sonnentag *et al.*, 2012):

$$166 \quad GCC = \frac{G_{DN}}{R_{DN} + B_{DN} + G_{DN}} \quad \text{Eqn 1.}$$

167 Where R_{DN}, B_{DN} and G_{DN} are the red, blue and green digital numbers of the image
168 respectively. Previous work has found a strong correlation between GCC and grassland
169 phenology including live biomass, leaf area index and aboveground gross primary production
170 (Migliavacca *et al.*, 2011, Toomey *et al.*, 2015). The GCC was calculated for each image
171 using R code available from <https://www.bitbucket.org/remkoduursma/phenora>.

172 A number of image quality checks were undertaken to exclude unsuitable images from the
173 analysis. Heavy rainfall occasionally flooded the rings, which obscured live vegetation and
174 increased the reflectance of light from the ground surface. We manually inspected images
175 taken during and after periods of heavy rainfall (i.e. > ~40 mm of precipitation over a 3-day

176 window) when flooding may have occurred. Images with evidence of flooding were
177 subsequently excluded from the analysis. A subset of photos from two plots within an eCO₂
178 treatment ring and one plot within an aCO₂ treatment ring were excluded due to the
179 encroachment of shrubs. Photos were excluded when shrub foliage cover exceeded ~20% of
180 the image region of interest, resulting in the removal of images beyond August 2015 and
181 November 2015 for the two respective eCO₂ plots and March 2017 for the aCO₂ plot.

182 Illumination and shadow affect the red-green-blue (RGB) brightness levels of an image, and
183 can consequently add unwanted variability in time series analysis of photos (Sonntag *et al.*,
184 2012). Although GCC has been shown to be less sensitive to the effects of scene illumination
185 than other indices (Sonntag *et al.*, 2012), additional controls were put in place to minimise
186 the effect of scene illumination and shadow. Images captured 10 minutes to 40 minutes
187 following sunrise were used for data analysis, as preliminary examination of data revealed
188 that images captured in this period provide a reliable estimate of GCC and are not impacted
189 by shadows (S1). Images with very low illumination were filtered out by excluding images
190 with a total RGB value less than 250. The 90th percentile value for each camera was then
191 calculated over a three day moving window (GCC_{90th}) in order to further minimise the effect
192 of daily scene illumination (Sonntag *et al.*, 2012).

193 Manual classification of live foliage cover was undertaken on a set of images taken from each
194 camera at four points in time (August 2014, February 2015, August 2015 and February
195 2016). Images captured towards the start and finish of the southern hemisphere growing
196 season were targeted as they coincide with the seasonal minima and maxima in understorey
197 cover. A 12 x 12 (n = 144) grid of regularly spaced survey points was generated across the
198 image region of interest (Fig. 1b) in ArcGIS (Esri, Redlands, CA). The substrate intersected
199 by each point was inspected on the screen and classified as (i) live foliage, (ii) dead foliage,
200 (iii) leaf litter, (iv) branches, twigs or bark, or (v) soil, by one operator (SV) to minimise bias.
201 The percentage of points classified as live vegetation was calculated and used as an estimate
202 of live foliage cover (%). GCC_{90th} was calculated for the region of interest in each photo
203 within three days of the photo capture. The relationship between live foliage cover and
204 GCC_{90th} was modelled using a linear mixed effect model, with camera and ring specified as
205 random effects. GCC_{90th} was found to be a good predictor of live foliage cover ($R^2 = 0.84$,
206 $F_{1,66} = 693.85$, $P < 0.001$, Fig. 2). The modelled relationship was used to estimate live foliage
207 cover for the GCC_{90th} time series (Live cover = $612.97GCC_{90th} - 189.01$).

208 Understorey biomass

209 Non-destructive estimates of understorey biomass were undertaken at the understorey plots
210 using plant height measurements obtained from stereo-photography. Stereo-photography has
211 been found to be a cost efficient and effective means to derive structural information for
212 plants, which can be utilised to estimate a range of plant attributes including vegetative
213 biomass (Yoon & Thai, 2010). A Bumblebee XB3 stereo video camera (Point Grey
214 Research) was used in our study, with details of camera specifications, settings and
215 calibration provided in S2. Plots were surveyed at one to three month intervals between
216 February 2015 and March 2017. Measurements were taken at dusk under diffuse light
217 conditions to avoid measurement errors related to shadows from trees and EucFACE
218 infrastructure on the understorey vegetation canopy. On each sampling date, three
219 consecutive measurements were taken over the centre of each understorey plot, from which
220 mean plant height (H_{mean} , in m) was calculated for each plot. Aboveground biomass (B , in
221 Kg m^{-2}) in each plot was estimated from mean plant height using an empirical model
222 developed for the grassy understorey vegetation at the EucFACE ($B = 1.72H_{mean} - 0.05$,
223 see S2); estimated aboveground biomass for each ring was calculated by averaging the four
224 plot estimates obtained for each ring.

225 Statistical analysis

226 Generalised Additive Mixed Models (GAMMs) were used to assess temporal patterns in live
227 foliage cover and biomass and the effect of CO_2 treatments and environmental parameters.
228 GAMMs utilise smoothing functions to link response and predictor variables, allowing for
229 estimation of non-linear relationships (Zuur *et al.*, 2009). Cubic regression splines were used
230 in all fitted GAMMs. The smoother term degrees of freedom were set at values that provide
231 biologically realistic representation of changes in live foliage cover and biomass (i.e. the
232 number of increasing and decreasing trends) over the study period.

233 Temporal patterns in understorey growth were initially plotted and visually compared with
234 daily trends in precipitation, volumetric water content (VWC) of soil and temperature. A
235 GAMM was fitted to the time series of live foliage cover, with the smoothed term in the
236 model (Time) allowed to have up to 25 degrees of freedom. Numerical derivatives of live
237 foliage cover (dC/dT) and confidence intervals were estimated from the GAMM and used to
238 identify any significant increase or decrease in live foliage cover (see Duursma *et al.*, 2016),

239 which represent periods of growth and senescence respectively. Daily precipitation was
240 obtained from the Australian Bureau of Meteorology (BOM) rain gauge at the EucFACE
241 facility (Station 67021, www.bom.gov.au, accessed 19th July 2017). Average daily VWC to
242 30 cm depth was calculated using data collected at 15 minute intervals from 48 soil moisture
243 probes (CS650-L; Campbell Scientific, Logan, UT, USA) located within the six experimental
244 rings (8 probes per ring). Daily temperature data was obtained from a BOM station located
245 ~5 km from EucFACE (Station 67105, www.bom.gov.au, accessed 19th July 2017).

246 GAMMs were fitted to the aCO₂ and eCO₂ subsets of the live foliage cover and biomass
247 datasets separately, with time since the commencement of the photo capture (Time) specified
248 as a smoother term and Ring as a random effect to account for repeated sampling within
249 Rings. The smoothed term (Time) was allowed to have up to 25 and 12 degrees of freedom
250 for live cover and biomass respectively, reflecting differences in the sampling frequency.
251 Model predictions and 95% confidence intervals were plotted to determine if CO₂ treatment
252 was leading to differences in live foliage cover and biomass over time. A linear mixed effect
253 model (LMM) was used to assess the statistical significance of the interaction between CO₂
254 treatment and Time, with Time and CO₂ being treated as fixed factors and Ring as a random
255 effect. Fitting of the LMM was restricted to dates when there was data available for all six
256 rings, which included 67% of the live foliage cover data and all of the biomass data. Residual
257 and quantile plots were visually assessed to determine if the assumptions of homogeneity of
258 variance and normality were met. Variance showed a fanning pattern as fitted values
259 increased for live foliage cover, so a square root transformation was applied and a power of
260 the covariate variance structure was added to allow variance to change with Time, to satisfy
261 the assumption of homogeneity of variance (Zuur *et al.*, 2009). A square root transformation
262 was applied to biomass and a constant variance function was included to allow different
263 variance for CO₂ treatment levels (Zuur *et al.*, 2009).

264 The effect of eCO₂ on vegetation cover and growth are often dependent upon water
265 availability across semi-arid and temperate systems. There was a strong spatial gradient in
266 soil VWC across EucFACE, which may result in spatial and temporal variability in CO₂
267 effects on vegetation growth that would be undetected in time series analysis. We tested
268 whether the relationship between soil VWC and live foliage cover and growth was effected
269 by eCO₂ by comparing GAMMs fitted with (i) a single smoother for VWC and (ii) smoothers
270 for VWC that were allowed to vary depending on CO₂ treatment. Data from the growing

271 season (August to March, Fig. 3a & b) was used for this analysis. The number of days since
272 the first of August (i.e. growing season start date, GSS) and tree canopy leaf area index (LAI)
273 were included as covariates in the GAMM. We favoured using GSS as a covariate over
274 temperature, because GSS will incorporate the effects of both temperature and photoperiod.
275 Overstorey LAI was estimated from measurements of below- and above-canopy PAR on
276 cloudy days, following Duursma *et al.* (2016). To generate daily values of overstorey LAI,
277 the data were interpolated using a smoother, as described by Duursma *et al.* (2016).

278 Vegetation and climatic time series data will have strong temporal auto-correlation (Zuur *et*
279 *al.*, 2009). In order to minimise the effect of autocorrelation in our analysis of growth we
280 sampled live foliage cover at 15-day intervals. A 15-day window was selected as it reflected a
281 time scale at which meaningful changes in foliage growth rates and VWC occurred (Fig. 3)
282 and it provided a fine enough sample frequency to capture a large range of environmental
283 conditions associated with GSS and LAI. Average values of VWC and LAI were calculated
284 for the 15 days preceding the live foliage cover measurement. Growth rate was calculated as
285 the change in live foliage cover between the start and end of the 15-day window. A GAMM
286 was initially fitted with smoothers for VWC, GSS and LAI and Ring as a random effect.
287 Smoothers were allowed to have up to 5 degrees of freedom. A semi-variogram was visually
288 assessed for evidence of temporal autocorrelation of residuals. There was evidence of
289 temporal auto-correlation of the residuals for live foliage cover, so data were resampled at 30
290 day intervals and a correlation structure (Spherical Correlation Structure) was added to the
291 GAMM in order to reduce auto-correlation of the residuals. Dependent variables that were
292 not statistically significant ($P > 0.05$) were dropped from the model to derive the most
293 parsimonious model containing significant effects. A fixed CO₂ term and separate VWC
294 smoothers for aCO₂ and eCO₂ were then added to the model and a likelihood ratio test was
295 used to compare the fit of the two models.

296 Analyses were undertaken using R version 3.4.1 (R Development Core Team, 2016).
297 GAMMs were fitted using the 'mgcv' package (Wood, 2006). LMMs were fitted using the
298 'nlme' package (Pinheiro *et al.*, 2017).

299 **Results**

300 **Environmental conditions and phenology**

301 Environmental conditions experienced at EucFACE varied considerably during the course of
302 the experiment (Fig. 3c & d). Total precipitation ranged from 587 mm to 631 mm across the
303 three growing seasons (August - March). However, precipitation events were sporadic,
304 resulting in extended dry periods during which soil VWC fell below $0.07 \text{ m}^3 \text{ m}^{-3}$ (Fig. 3c),
305 which have been shown to reduce CO_2 assimilation of the dominant C3 grasses by ~30% -
306 50% at EucFACE (Pathare *et al.*, 2017). These dry periods were generally associated with
307 declining live foliage cover during our study (e.g. Nov 2014, Mar 2015, Apr – Jun 2016, Nov
308 – Dec 2016; Fig. 3a & b). Periods of high water availability ($\text{VWC} > 0.2 \text{ m}^3 \text{ m}^{-3}$) occurred
309 periodically during both the warm and cool months (i.e. Apr – Sept 2015, Jan – Feb 2016,
310 Jun – Sep 2016, Mar 2017; Fig. 3c & d). Maximum daily temperature ranged between 11.8°C
311 and 47.0°C (Fig. 3d), with a mean maximum temperature of 30.8°C during summer and
312 18.5°C during winter. Maximum daily temperature exceeded 33.9°C on 25% of days during
313 summer and heatwaves with several days exceeding 40.0°C were not uncommon (e.g. Nov
314 2015, Jan 2017; Fig. 3d). Minimum daily temperatures ranged between -2.5°C and 14.3°C
315 (Fig. 3d), with a mean minimum temperature of 5.3°C .

316 Patterns of understorey growth varied across growing seasons (Fig. 3a & b), reflecting
317 patterns in both temperature and water availability. The onset of growth typically commenced
318 in August, as indicated by the increasing trend in live foliage cover (Fig. 3a) and the
319 significant positive response in the first derivative (dC/dt) of the GAMM (Fig. 3b). The end
320 of the growing season was not as distinct, with live foliage cover declining gradually over the
321 Autumn and Winter months in both years (Fig. 3a & b), though periods of growth were
322 uncommon after the end of March (Fig. 3b). Multimodal growth patterns occurred over each
323 growing season (August – March) which was associated with soil VWC (Fig. 3). Despite
324 different patterns in the timing and amount of rainfall in each growing season, maximum
325 foliage cover always reached ~40%, with the exception of a spike in March 2017 which was
326 driven by the growth of annual forbs (Fig. 3a).

327 Rapid understorey senescence was observed during two heatwaves that occurred under
328 conditions of water limitation ($\text{VWC} < 0.1 \text{ m}^3 \text{ m}^{-3}$; Inset 1 and 4, Fig. 3a). Both heatwaves
329 were followed by rainfall events that facilitated rapid re-growth (Fig. 3), highlighting the

330 capacity for rapid recovery of understorey biomass in these ecosystems. Psyllid infestations
331 resulted in periodic defoliation of tree canopies throughout the study (Fig. 3a) (Gherlenda *et*
332 *al.*, 2016), leading to increased photosynthetically active radiation (PAR) reaching the
333 understorey (Duursma *et al.*, 2016). This led to exceptionally high live understorey foliage
334 cover values recorded during January – February 2015 (Inset 2, Fig. 3a) and may have
335 contributed to rapid growth in Spring 2015 (See arrow in Fig. 3a).

336 **Effects of eCO₂ on live foliage cover and biomass**

337 There was no effect of CO₂ treatment on either live foliage cover or biomass over the
338 duration of the experiment, as evidenced by a consistent overlap of the estimated 95%
339 confidence interval from the fitted GAMMs (i.e. $P > 0.05$ at any given time, Fig. 4). A LMM
340 found no significant interaction between date of measurement (Time) and CO₂ treatment for
341 both cover and biomass (Table 1), providing support for this observation. However, we do
342 note that mean biomass (\pm 95% confidence interval) in the aCO₂ plots ($0.345 \pm 0.028 \text{ Kg m}^{-2}$)
343 was generally greater than in the eCO₂ plots ($0.312 \pm 0.037 \text{ Kg m}^{-2}$), with a difference of
344 $0.032 \pm 0.019 \text{ Kg m}^{-2}$ across the measurement periods. There was considerable variability in
345 both cover and biomass within CO₂ treatments at any given point in time, which likely
346 reflects gradients in environmental conditions (e.g. soil VWC) across the EucFACE site.

347 **Effects of climate and eCO₂ on live foliage cover**

348 Soil VWC was the only significant predictor of growth rate ($F_{2, 224} = 8.2349$, $P = 0.0004$, R^2
349 $= 0.14$), whereby growth rate showed a hump-shaped relationship with soil VWC, peaking at
350 $\sim 0.15 \text{ m}^3 \text{ m}^{-3}$ (Fig. 5). When VWC fell below $\sim 0.06 \text{ m}^3 \text{ m}^{-3}$ declines in live foliage cover were
351 recorded (Fig. 5), indicating periods of senescence. Patterns in live foliage cover were
352 significantly affected by soil VWC and time since the growing season start date (GSS) ($F_{3, 123}$
353 $= 109.7660$, $P < 0.0001$, $R^2 = 0.40$; S3). Live foliage cover showed an asymptotic
354 relationship with water availability late in the growing season, increasing with soil VWC up
355 to $\sim 0.1 \text{ m}^3 \text{ m}^{-3}$ then levelling off (Fig. 6). A similar relationship was evident for GSS when
356 soil VWC exceeded $\sim 0.15 \text{ m}^3 \text{ m}^{-3}$, whereby foliage cover increased up to 150 days from the
357 growing season start date and levelled off thereafter (Fig. 6). Model predictions indicate
358 greatest live foliage cover occurs late in the growing season when soil VWC exceeds ~ 0.10
359 $\text{m}^3 \text{ m}^{-3}$ (Fig. 6).

360 Comparison of models with and without unique VWC smoothers for the CO₂ treatments
361 showed that allowing smoothers to vary did not improve the model goodness of fit for live
362 foliage cover ($L = 2.5457$, $df = 3$, $P = 0.4671$) or growth rate ($L = 0.4988$, $df = 3$, $P =$
363 0.9192). These analyses indicate that eCO₂ did not modify the effect of VWC on growth and
364 cover, hence there is no evidence that eCO₂ increased live foliage cover or growth rates
365 during periods of low soil moisture.

366 Discussion

367 Our experiment provides the first field based assessment of the interactive effect of eCO₂ and
368 water availability on understorey productivity in a grassy woodland ecosystem. Through the
369 use of repeat near-surface digital photography we were able to quantify short term responses
370 (weekly – monthly) of understorey cover and biomass, and assess the effect of eCO₂ during
371 periods of varying water availability. Climatic conditions experienced during the ~2.5 year
372 study included growing seasons with extended periods of water limitation ($VWC < 0.07 \text{ m}^3$
373 m^{-3}), sufficient to reduce the rate of photosynthesis of the dominant herbaceous species at the
374 site (Pathare *et al.*, 2017). Water availability was the dominant driver of understorey
375 productivity, with low understorey growth rates and cover being recorded under conditions of
376 low soil water availability, as has been found in grasslands globally (Del Grosso *et al.*, 2008,
377 Hovenden *et al.*, 2014, Morgan *et al.*, 2004, Reich *et al.*, 2014). Contrary to expectations,
378 eCO₂ did not increase understorey productivity during periods of water limitation. This is
379 surprising as water savings associated with eCO₂ have consistently been found to increase
380 grassland productivity by alleviating water stress in semi-arid and temperate environments
381 (Hovenden *et al.*, 2014, Morgan *et al.*, 2011, Morgan *et al.*, 2004, Reyes-Fox *et al.*, 2014,
382 Smith *et al.*, 2000, Zhu *et al.*, 2016a). Our findings suggest that any effect of eCO₂ on
383 herbaceous understorey productivity was much smaller than the effect of climate variability.
384 Consequently, future increases in [CO₂] may not offset the effect of future drying on
385 understorey productivity in temperate grassy woodlands of Australia.

386 Although canopy trees at EucFACE have exhibited reduced stomatal conductance in response
387 to eCO₂ (Drake *et al.*, 2016, Gimeno *et al.*, 2016), with no concurrent effect of eCO₂ on
388 canopy LAI (Duursma *et al.*, 2016), there has been no eCO₂ treatment effect on stomatal
389 conductance for the dominant C3 herbaceous understorey plants (Pathare *et al.*, 2017). VWC
390 in the upper 30 cm of the soil profile at EucFACE has not increased in response to eCO₂
391 (Pathare *et al.*, 2017), which is one likely explanation for the absence of eCO₂ stimulation of

392 understory productivity during periods of water limitation. However, carbon assimilation
393 (A_{net}) in the C3 herbaceous understory plants at EucFACE did increase by ~30% under
394 $e\text{CO}_2$, with the greatest stimulation occurring during periods of low water availability
395 (Pathare *et al.*, 2017). It is possible that extra assimilated carbon is being invested into below
396 ground growth of grasses (Suter *et al.*, 2002), which cannot be resolved using the remote
397 sensing techniques employed in our study. Increased allocation of carbon to roots has been
398 observed for grasses grown under $e\text{CO}_2$ in the absence of nutrient addition (e.g. N, Suter *et*
399 *al.*, 2002). Previous studies have documented that N availability decreases in $e\text{CO}_2$ (e.g.
400 Reich *et al.*, 2006) but the lack of response in our site may have been, at least partially, driven
401 by a putative P-deficiency (see Ellsworth *et al.*, 2017), although detailed discussions are
402 beyond scope. Alternatively, the absence of growth response to $e\text{CO}_2$ may reflect light
403 limitations in the understory. Gas exchange measurements conducted by Pathare *et al.*
404 (2017) used saturating light levels ($1800 \mu\text{mol m}^{-2} \text{s}^{-1}$), in order to simulate maximum C
405 assimilation during periodic (30 mins/day) sun flecks in Spring and Summer. Consequently,
406 competition for light with trees may potentially explain the different growth response
407 between the woodland understory examined in our study and temperate grasslands
408 elsewhere (e.g. Hovenden *et al.*, 2014, Morgan *et al.*, 2004, Reyes-Fox *et al.*, 2014).

409 A key advantage of the application of near-surface remote sensing is the ability to detect
410 short-term responses in above ground productivity in response to environmental change,
411 which cannot be characterised by annual measures of growth (Hufkens *et al.*, 2016, Zelikova
412 *et al.*, 2015). Using this approach we were able to quantify temporal patterns in understory
413 productivity and detect thresholds in VWC that were associated with understory mortality
414 ($<0.06 \text{ m}^3 \text{ m}^{-3}$) and peak growth rates ($\sim 0.1 - 0.2 \text{ m}^3 \text{ m}^{-3}$), which correspond to periods of
415 minimum and maximum CO_2 assimilation for the dominant herbaceous plants in the study
416 area (Pathare *et al.*, 2017). The hump shaped response of understory growth to soil water
417 availability was not entirely unexpected, reflecting the effects of water limitations during
418 periods of low VWC and changes to environmental conditions associated with high VWC
419 (Zhu *et al.*, 2016a). Substantial volumes of rainfall ($>120 \text{ mm}$ in 7 days) are needed to
420 increase surface VWC beyond $0.2 \text{ m}^3 \text{ m}^{-3}$ at EucFACE, with periods of consistent rainfall
421 (i.e. weeks) required to sustain high surface VWC (Fig. 3c). Consequently, periods of high
422 VWC are typically associated with cloudy conditions, which lead to lower growth rates due
423 to light limitation. Nutrient leaching may have also contributed to low growth rates under
424 very wet conditions, though such effects may vary seasonally (Hovenden *et al.*, 2014).

425 Productivity of the understorey community was resilient to the effects of environmental
426 variability, displaying the ability for rapid recovery following periodic drought and
427 heatwaves (Inset 1 and 4, Fig. 3a). Rapid recovery of cover and biomass in native Australian
428 temperate grasslands following drought has been demonstrated in a number of experiments
429 (Mitchell *et al.*, 2016, Power *et al.*, 2016), facilitated by the ability for vegetative regrowth of
430 dominant native grasses, such as *M. stipoides* (Mitchell *et al.*, 2016). Total growing season
431 precipitation was relatively consistent across years, though the timing of wet and dry cycles
432 within growing seasons varied. The maximum cover and biomass recorded within each year
433 was reasonably consistent, suggesting that above ground productivity may be insensitive to
434 the timing of water limitation during the growing season, unlike some temperate grasslands
435 (Craine *et al.*, 2012, Hovenden *et al.*, 2014). This observation is supported by experimental
436 manipulations using herbaceous species common to Australian temperate grasslands and
437 woodlands, which show that aboveground productivity of the understorey responds to the
438 amount of precipitation over the growing season, not the timing of rainfall events within the
439 growing season (Gibson-Forty *et al.*, 2016, Power *et al.*, 2016). Continued monitoring at
440 EucFACE will provide further insight into the effects of rainfall variability on the dynamics
441 of understorey growth and the potential for temporal lags in growth response to water
442 availability (i.e. legacy effects; Sala *et al.*, 2012).

443 Productivity has been observed to increase in response to climate change in some grasslands,
444 with higher temperatures leading to earlier Spring growth and eCO₂ effectively extending the
445 growing season by increasing plant water use efficiency (Barichivich *et al.*, 2013, Hufkens *et*
446 *al.*, 2016, Reyes-Fox *et al.*, 2014). However, our results suggest that trends of declining grass
447 productivity may occur in Australian temperate grassy woodlands under future climate. A
448 drying trend is projected for temperate regions of Australia, with declines (~20 - 30%) in
449 winter and spring precipitation and increases in the number of days spent in drought expected
450 by the end of the century (CSIRO and Bureau of Meteorology, 2015). Although rising
451 temperatures will result in earlier onset of Spring growth, lower Spring precipitation and
452 increased frequency of Summer droughts will likely result in reduced understorey
453 productivity. Consequently, the understorey growth response of grassy woodland ecosystems
454 to future climate across temperate regions in Australia may not contribute towards the
455 mitigation of rising atmospheric [CO₂], contrary to predictions for many other ecosystems
456 (e.g. Hufkens *et al.*, 2016).

457 The importance of indirect effects of invertebrate herbivores on canopy – understory
458 interactions was evident in our study. Psyllids are common agents of periodic canopy
459 senescence within eucalypts across Australian forests and woodlands (Gherlenda *et al.*,
460 2016). Two major psyllid overstorey defoliation events occurred during the study period,
461 driven by the leaf senescence-inducing *Cardiaspina fiscella* (Gherlenda *et al.*, 2016), which
462 subsequently resulted in increased productivity of understory vegetation (Fig. 3a).
463 Defoliation of trees in Ring 6 during November and December 2014 resulted in increased
464 photosynthetically active radiation (PAR) reaching the understory (Duursma *et al.*, 2016),
465 which along with sufficient soil water availability, contributed to the exceptionally high
466 understory live foliage cover recorded in the understory during January – February 2015
467 (Inset 2, Fig. 3a). A subsequent Psyllid outbreak affecting the entire study area occurred at
468 the onset of the 2015/2016 growing season (See arrow in Fig. 3a), though it is difficult to
469 discern to what degree the rapid growth was due to suitable climatic conditions, increased
470 PAR or the combination of both. These observations suggest that climate-herbivore
471 interactions will be influential in determining ecosystem productivity and ecosystem carbon
472 exchange, as has been observed in other ecosystems (Allen *et al.*, 2010, Keith *et al.*, 2012).

473 Predicted shifts towards greater aridity and more frequent drought in semi-arid, temperate
474 and tropical regions of the globe (CSIRO and Bureau of Meteorology, 2015, IPCC, 2014) are
475 likely to modify herbaceous productivity across large areas of the grassland, woodland and
476 savanna biomes (Hufkens *et al.*, 2016, Lehmann *et al.*, 2014, Zhu *et al.*, 2016a). While water
477 savings associated with increasing [CO₂] have the potential to offset the effects of increasing
478 aridity on grass productivity (Reyes-Fox *et al.*, 2014), these effects are not ubiquitous
479 (Morgan *et al.*, 2004, Reich *et al.*, 2014, Zelikova *et al.*, 2015), as further demonstrated in our
480 study. Future climate change could lead to lower understory productivity in Australian
481 temperate grassy woodlands, via reductions to Spring rainfall and increasing drought.
482 However, the sensitivity of these systems to total precipitation suggest large inter-annual
483 variability in grass productivity is likely, as has been suggested for other ecosystems globally
484 (e.g. Zhu *et al.*, 2016a). Climate change and biotic interactions such as herbivory are likely to
485 exert much greater influence on understory productivity than increased atmospheric [CO₂]
486 in temperate grassy woodlands.

487 Acknowledgements

488 We thank Steven Wohl, Vinod Kumar, Craig Barton and Craig McNamara for maintaining
489 the FACE facility. Vinod Kumar, Craig McNamara, Eli Bendall and Corey Anderson assisted
490 with photo collection and camera maintenance. Alex Robertson assisted with stereo camera
491 measurements. Steven Wohl and Vinod Kumar assisted with the design and installation of the
492 camera housings. The EucFACE experiment is funded by the Australian Government,
493 through the Education Investment Fund, the Department of Industry and Science and the
494 Australian Research Council, and Western Sydney University. Funding for the cameras and
495 data analysis was provided by Australian Research Council Discovery Grant number
496 130102576. The stereo camera and application development was funded by the Western
497 Sydney University Internal Research Scheme. VRD acknowledges funding from a Ramón y
498 Cajal fellowship (RYC-2012-10970). The raw data used in this manuscript are publically
499 available (doi: 10.6084/m9.figshare.5721079).

500 References

- 501 Ainsworth EA, Long SP (2005) What have we learned from 15 years of free-air CO₂
502 enrichment (FACE)? A meta-analytic review of the responses of photosynthesis,
503 canopy properties and plant production to rising CO₂. *New Phytologist*, **165**, 351-372.
- 504 Allen CD, Macalady AK, Chenchouni H *et al.* (2010) A global overview of drought and heat-
505 induced tree mortality reveals emerging climate change risks for forests. *Forest
506 Ecology and Management*, **259**, 660-684.
- 507 Asner GP, Elmore AJ, Olander LP, Martin RE, Harris AT (2004) Grazing systems,
508 ecosystem responses, and global change. *Annual Review of Environment and
509 Resources*, **29**, 261-299.
- 510 Ballantyne AP, Alden CB, Miller JB, Tans PP, White JWC (2012) Increase in observed net
511 carbon dioxide uptake by land and oceans during the past 50 years. *Nature*, **488**, 70-
512 72.
- 513 Barichivich J, Briffa KR, Myneni RB *et al.* (2013) Large-scale variations in the vegetation
514 growing season and annual cycle of atmospheric CO₂ at high northern latitudes from
515 1950 to 2011. *Global Change Biology*, **19**, 3167-3183.

516 Bond WJ, Midgley GF (2012) Carbon dioxide and the uneasy interactions of trees and
517 savannah grasses. *Philosophical Transactions of the Royal Society of London B:*
518 *Biological Sciences*, **367**, 601-612.

519 Craine JM, Nippert JB, Elmore AJ, Skibbe AM, Hutchinson SL, Brunsell NA (2012) Timing
520 of climate variability and grassland productivity. *Proceedings of the National*
521 *Academy of Sciences*, **109**, 3401-3405.

522 CSIRO and Bureau of Meteorology (2015) *Climate Change in Australia Information for*
523 *Australia's Natural Resource Management Regions: Technical Report*, Australia,
524 CSIRO and Bureau of Meteorology,.

525 Del Grosso S, Parton W, Stohlgren T *et al.* (2008) Global potential net primary production
526 predicted from vegetation class, precipitation, and temperature. *Ecology*, **89**, 2117-
527 2126.

528 Donohue RJ, Roderick ML, McVicar TR, Farquhar GD (2013) Impact of CO₂ fertilization on
529 maximum foliage cover across the globe's warm, arid environments. *Geophysical*
530 *Research Letters*, **40**, 3031-3035.

531 Drake JE, Macdonald CA, Tjoelker MG *et al.* (2016) Short-term carbon cycling responses of
532 a mature eucalypt woodland to gradual stepwise enrichment of atmospheric CO₂
533 concentration. *Global Change Biology*, **22**, 380-390.

534 Duursma RA, Gimeno TE, Boer MM, Crous KY, Tjoelker MG, Ellsworth DS (2016) Canopy
535 leaf area of a mature evergreen Eucalyptus woodland does not respond to elevated
536 atmospheric [CO₂] but tracks water availability. *Global Change Biology*, **22**, 1666-
537 1676.

538 Ellsworth DS, Anderson IC, Crous KY *et al.* (2017) Elevated CO₂ does not increase eucalypt
539 forest productivity on a low-phosphorus soil. *Nature Clim. Change*, **7**, 279-282.

540 Gherlenda AN, Esveld JL, Hall AAG, Duursma RA, Riegler M (2016) Boom and bust: rapid
541 feedback responses between insect outbreak dynamics and canopy leaf area impacted
542 by rainfall and CO₂. *Global Change Biology*, **22**, 3632-3641.

543 Gibson-Forty EVJ, Barnett KL, Tissue DT, Power SA (2016) Reducing rainfall amount has a
544 greater negative effect on the productivity of grassland plant species than reducing
545 rainfall frequency. *Functional Plant Biology*, **43**, 380-391.

546 Gimeno TE, Crous KY, Cooke J, O'Grady AP, Ósvaldsson A, Medlyn BE, Ellsworth DS
547 (2016) Conserved stomatal behaviour under elevated CO₂ and varying water
548 availability in a mature woodland. *Functional Ecology*, **30**, 700-709.

- 549 Hovenden MJ, Newton PCD, Wills KE (2014) Seasonal not annual rainfall determines
550 grassland biomass response to carbon dioxide. *Nature*, **511**, 583-586.
- 551 Hufkens K, Keenan TF, Flanagan LB *et al.* (2016) Productivity of North American
552 grasslands is increased under future climate scenarios despite rising aridity. *Nature*
553 *Clim. Change*, **6**, 710–714.
- 554 IPCC (2014) *Climate Change 2014: Mitigation of Climate Change. Contribution of Working*
555 *Group III to the Fifth Assessment Report of the Intergovernmental Panel on Climate*
556 *Change*, Cambridge, United Kingdom, Cambridge University Press.
- 557 Keith H, van Gorsel E, Jacobsen KL, Cleugh HA (2012) Dynamics of carbon exchange in a
558 Eucalyptus forest in response to interacting disturbance factors. *Agricultural and*
559 *Forest Meteorology*, **153**, 67-81.
- 560 Kolby Smith W, Reed SC, Cleveland CC *et al.* (2016) Large divergence of satellite and Earth
561 system model estimates of global terrestrial CO₂ fertilization. *Nature Clim. Change*, **6**,
562 306-310.
- 563 Lehmann CER, Anderson TM, Sankaran M *et al.* (2014) Savanna vegetation-fire-climate
564 relationships differ among continents. *Science*, **343**, 548-552.
- 565 Lehmann CER, Archibald SA, Hoffmann WA, Bond WJ (2011) Deciphering the distribution
566 of the savanna biome. *New Phytologist*, **191**, 197-209.
- 567 Lunt ID, Prober SM, Morgan JW (2012) How do fire regimes affect ecosystem structure,
568 function and diversity in grasslands and grassy woodlands of southern Australia? In:
569 *Flammable Australia: Fire Regimes, Biodiversity and Ecosystems in a Changing*
570 *World*. (eds Bradstock RA, Gill AM, Williams RJ) pp 253-270. Melbourne, CSIRO
571 Publishing.
- 572 Ma X, Huete A, Moran S, Ponce-Campos G, Eamus D (2015) Abrupt shifts in phenology and
573 vegetation productivity under climate extremes. *Journal of Geophysical Research:*
574 *Biogeosciences*, **120**, 2036-2052.
- 575 Migliavacca M, Galvagno M, Cremonese E *et al.* (2011) Using digital repeat photography
576 and eddy covariance data to model grassland phenology and photosynthetic CO₂
577 uptake. *Agricultural and Forest Meteorology*, **151**, 1325-1337.
- 578 Mitchell ML, Virgona JM, Jacobs JL, Kemp DR (2016) Summer drought survival and
579 recovery in *Microlaena stipoides*. *The Rangeland Journal*, **38**, 501-510.
- 580 Moore CE, Brown T, Keenan TF *et al.* (2016) Reviews and syntheses: Australian vegetation
581 phenology: new insights from satellite remote sensing and digital repeat photography.
582 *Biogeosciences*, **13**, 5085-5102.

583 Morgan JA, LeCain DR, Pendall E *et al.* (2011) C4 grasses prosper as carbon dioxide
584 eliminates desiccation in warmed semi-arid grassland. *Nature*, **476**, 202-205.

585 Morgan JA, Pataki DE, Körner C *et al.* (2004) Water relations in grassland and desert
586 ecosystems exposed to elevated atmospheric CO₂. *Oecologia*, **140**, 11-25.

587 Pathare VS, Crous KY, Cooke J, Creek D, Ghannoum O, Ellsworth DS (2017) Water
588 availability affects seasonal CO₂-induced photosynthetic enhancement in herbaceous
589 species in a periodically dry woodland. *Global Change Biology*, **23**, 5164–5178.

590 Pinheiro J, Bates D, DebRoy S, Sarkar D, R Core Team (2017) *nlme: Linear and Nonlinear*
591 *Mixed Effects Models*, R package version 3.1-131, [http://CRAN.R-](http://CRAN.R-project.org/package=nlme)
592 [project.org/package=nlme](http://CRAN.R-project.org/package=nlme).

593 Power SA, Barnett KL, Ochoa-Hueso R *et al.* (2016) DRI-Grass: A new experimental
594 platform for addressing grassland ecosystem responses to future precipitation
595 scenarios in south-east Australia. *Frontiers in Plant Science*, **7**, 1373.

596 R Development Core Team (2016) R: A language and environment for statistical computing.
597 Vienna, Austria, R Foundation for Statistical Computing.

598 Reich PB, Hobbie SE, Lee T *et al.* (2006) Nitrogen limitation constrains sustainability of
599 ecosystem response to CO₂. *Nature*, **440**, 922.

600 Reich PB, Hobbie SE, Lee TD (2014) Plant growth enhancement by elevated CO₂ eliminated
601 by joint water and nitrogen limitation. *Nature Geoscience*, **7**, 920-924.

602 Reyes-Fox M, Steltzer H, Trlica MJ, McMaster GS, Andales AA, LeCain DR, Morgan JA
603 (2014) Elevated CO₂ further lengthens growing season under warming conditions.
604 *Nature*, **510**, 259-262.

605 Sala OE, Gherardi LA, Reichmann L, Jobbágy E, Peters D (2012) Legacies of precipitation
606 fluctuations on primary production: theory and data synthesis. *Philosophical*
607 *Transactions of the Royal Society B: Biological Sciences*, **367**, 3135-3144.

608 Smith SD, Huxman TE, Zitzer SF *et al.* (2000) Elevated CO₂ increases productivity and
609 invasive species success in an arid ecosystem. *Nature*, **408**, 79-82.

610 Sonnentag O, Hufkens K, Teshera-Sterne C *et al.* (2012) Digital repeat photography for
611 phenological research in forest ecosystems. *Agricultural and Forest Meteorology*, **152**,
612 159-177.

613 Suter D, Frehner M, Fischer BU, Nösberger J, Lüscher A (2002) Elevated CO₂ increases
614 carbon allocation to the roots of *Lolium perenne* under free-air CO₂ enrichment but
615 not in a controlled environment. *New Phytologist*, **154**, 65-75.

616 Toomey M, Friedl MA, Frohling S *et al.* (2015) Greenness indices from digital cameras
617 predict the timing and seasonal dynamics of canopy-scale photosynthesis. *Ecological*
618 *Applications*, **25**, 99-115.

619 Wood SN (2006) *Generalized Additive Models: An Introduction with R.*, Chapman and
620 Hall/CRC.

621 Yoon SC, Thai CN (2010) Stereo Spectral Imaging System for Plant Health Characterization.
622 In: *Technological Developments in Networking, Education and Automation.* (eds
623 Elleithy K, Sobh T, Iskander M, Kapila V, Karim MA, Mahmood A) pp 181-186.
624 Dordrecht, Springer Netherlands.

625 Zelikova TJ, Williams DG, Hoenigman R, Blumenthal DM, Morgan JA, Pendall E (2015)
626 Seasonality of soil moisture mediates responses of ecosystem phenology to elevated
627 CO₂ and warming in a semi-arid grassland. *Journal of Ecology*, **103**, 1119-1130.

628 Zhu K, Chiariello NR, Tobeck T, Fukami T, Field CB (2016a) Nonlinear, interacting
629 responses to climate limit grassland production under global change. *Proceedings of*
630 *the National Academy of Sciences*, **113**, 10589-10594.

631 Zhu Z, Piao S, Myneni RB *et al.* (2016b) Greening of the Earth and its drivers. *Nature Clim.*
632 *Change*, **6**, 791-795.

633 Zuur A, Ieno EN, Walker N, Saveliev AA, Smith GM (2009) *Mixed Effects Models and*
634 *Extensions in Ecology with R*, New York, Springer.

635

636 Tables

637 **Table 1** Summary of linear mixed effect models testing the effects of [CO₂] and Time on the
638 cover and biomass of understorey vegetation. Cover and biomass were square root
639 transformed to satisfy the assumption of homogeneity of variance.

Response variable	Predictor variable	<i>F</i>	DF	DFres	<i>P</i> -value
Cover	Intercept	760.64	1	848	< 0.0001
	Time	36.56	212	848	< 0.0001
	CO ₂	0.30	1	4	0.6144
	Time x CO ₂	0.82	212	848	0.9650
Biomass	Intercept	660.42	1	68	< 0.0001

Time	7.61	17	68	<0.0001
CO ₂	0.54	1	4	0.5040
Time x CO ₂	0.70	17	68	0.7943

640

641

642 Figures

643 **Fig. 1** (a) Camera set up and (b) 1.5 m² (1.23 m x 1.23 m) region of interest (shaded red) used
644 for analysis across all photos

645 **Fig. 2** The fitted relationship (\pm 95% confidence interval) between GCC_{90th} and understorey
646 live foliage cover (%). The open grey circles and grey crosses are the observations used to fit
647 the LMM from winter and summer respectively. The shaded area is the 95% confidence
648 interval.

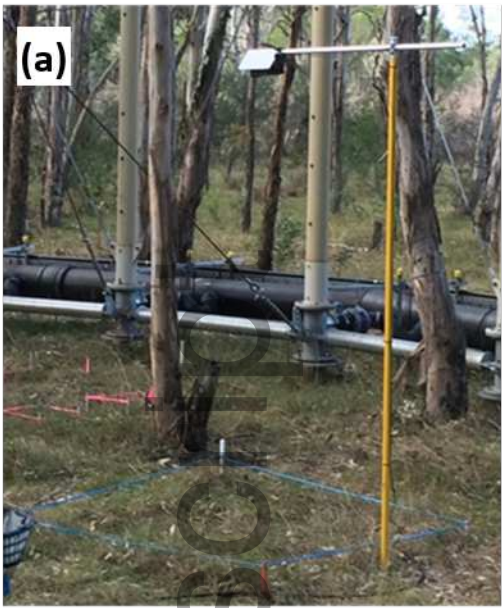
649 **Fig. 3** (a) Smoothed time series of understorey live foliage cover (%) averaged across all six
650 treatment rings. Box 1 and Box 4 depict episodes of grass curing triggered by extreme
651 temperatures and water deficit. Box 2 depicts the effects of overstorey canopy defoliation in
652 Ring 6 (ambient CO₂) due to Psyllids. Arrow 3 identifies the onset of Psyllid defoliation of
653 overstorey trees across all Rings. (b) Change in understorey live foliage cover (dC/dt),
654 including the 95% confidence intervals (shaded grey polygon). (c) Time series of daily
655 precipitation (black bars) and site level averages of soil volumetric water content (VWC)
656 (grey line). (d) Time series of daily maximum temperature (black points) and minimum
657 temperature (grey points).

658 **Fig. 4** (a) Mean understorey live foliage cover (%) and (b) biomass (Kg m⁻²) for the fitted
659 GAMMs for aCO₂ (blue line) and eCO₂ (red line). Points are the observed data for aCO₂
660 (blue) and eCO₂ (red). Shaded areas are the 95% confidence intervals.

661 **Fig. 5** Smooth regression models (black lines) for trends in understorey growth rate as a
662 function of mean soil VWC. The grey polygon represents the 95% confidence interval. Mean
663 values for VWC were calculated for the 15 days prior to the growth rate measurement date.

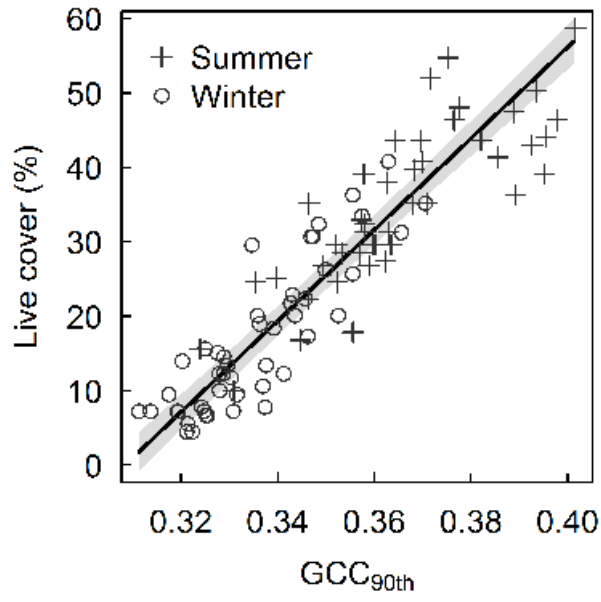
664 **Fig. 6** A contour plot showing the effect of days since the start of the growing season and
665 mean soil VWC ($\text{m}^3 \text{m}^{-3}$) on understorey live foliage cover (%). Values are based on
666 predictions from a GAMM. Mean values for VWC were made over a 15 day period prior to
667 the live foliage cover measurement.

Author Manuscript

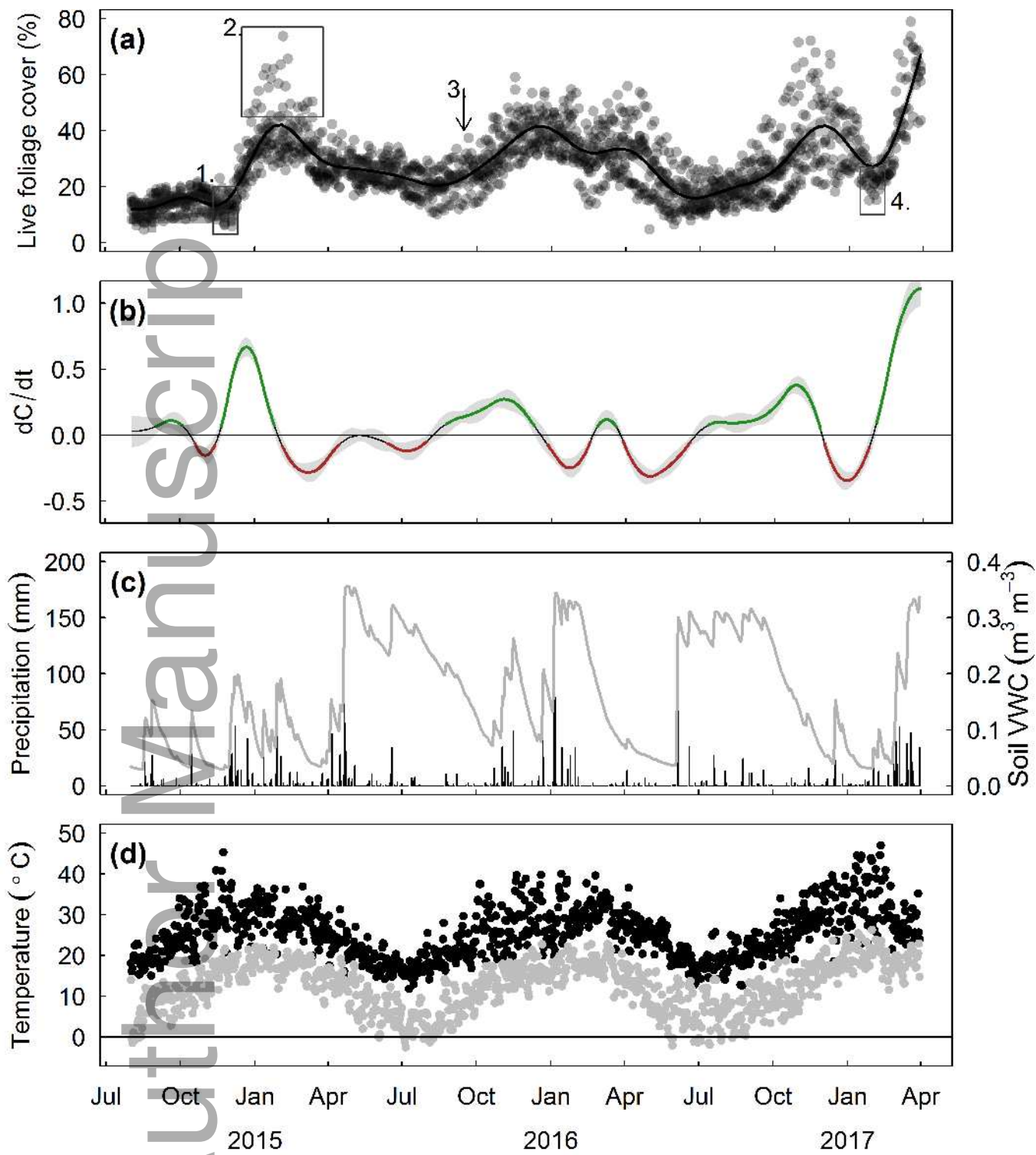


gcb_14038_f1.png

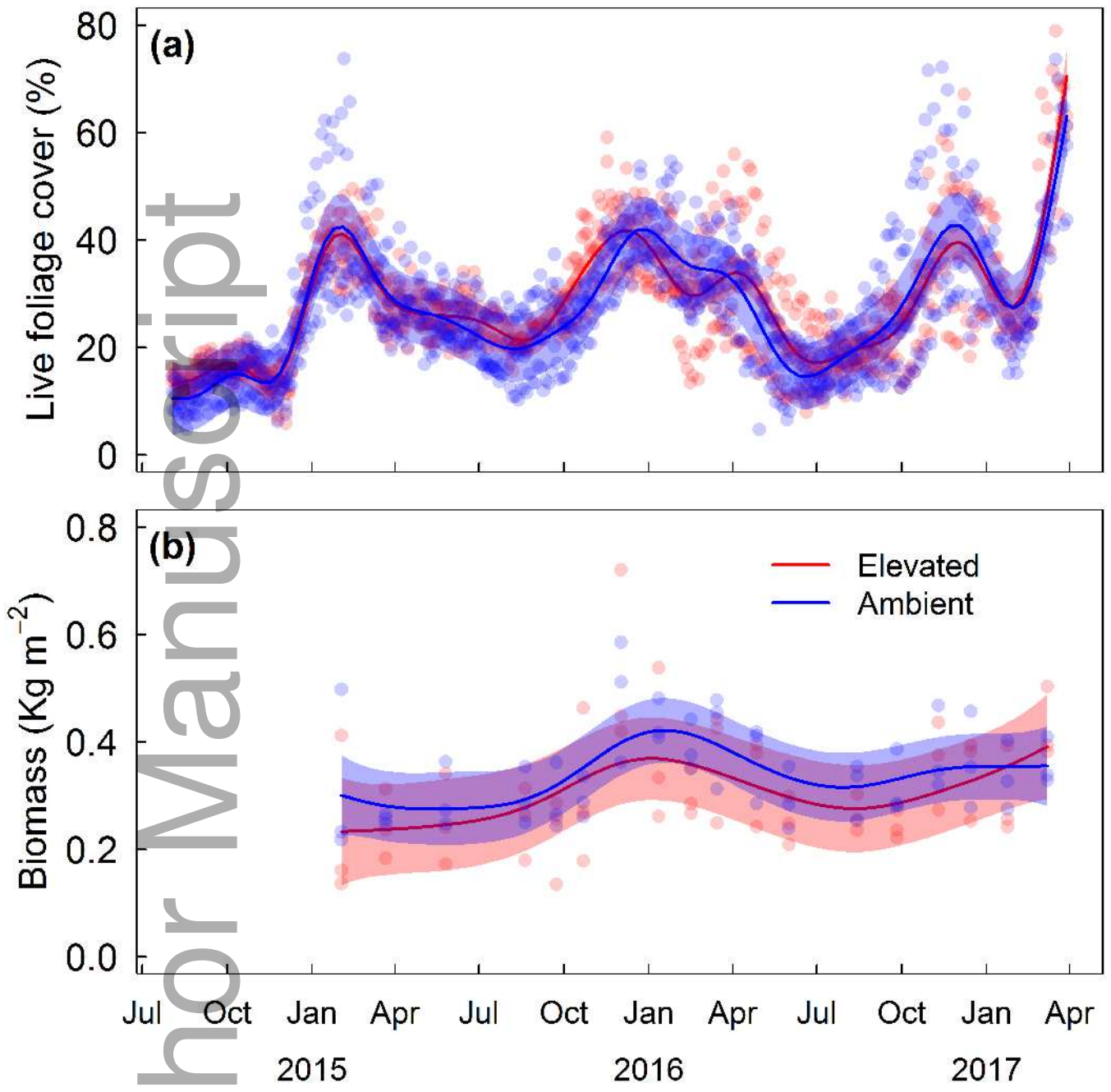
Author Manuscript



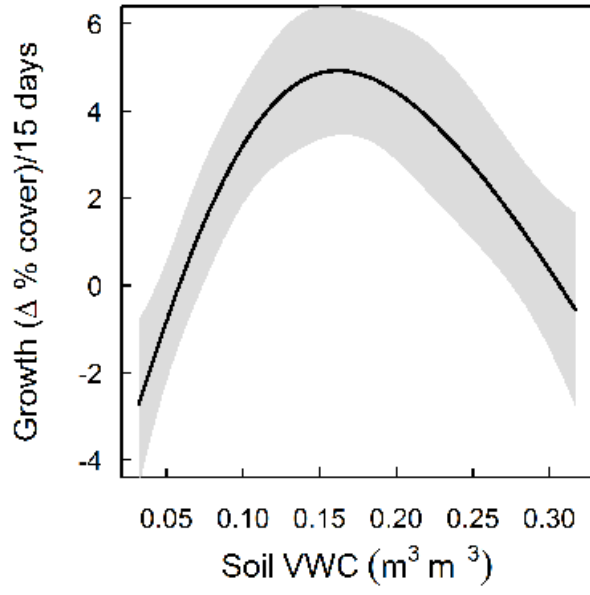
gcb_14038_f2.tiff



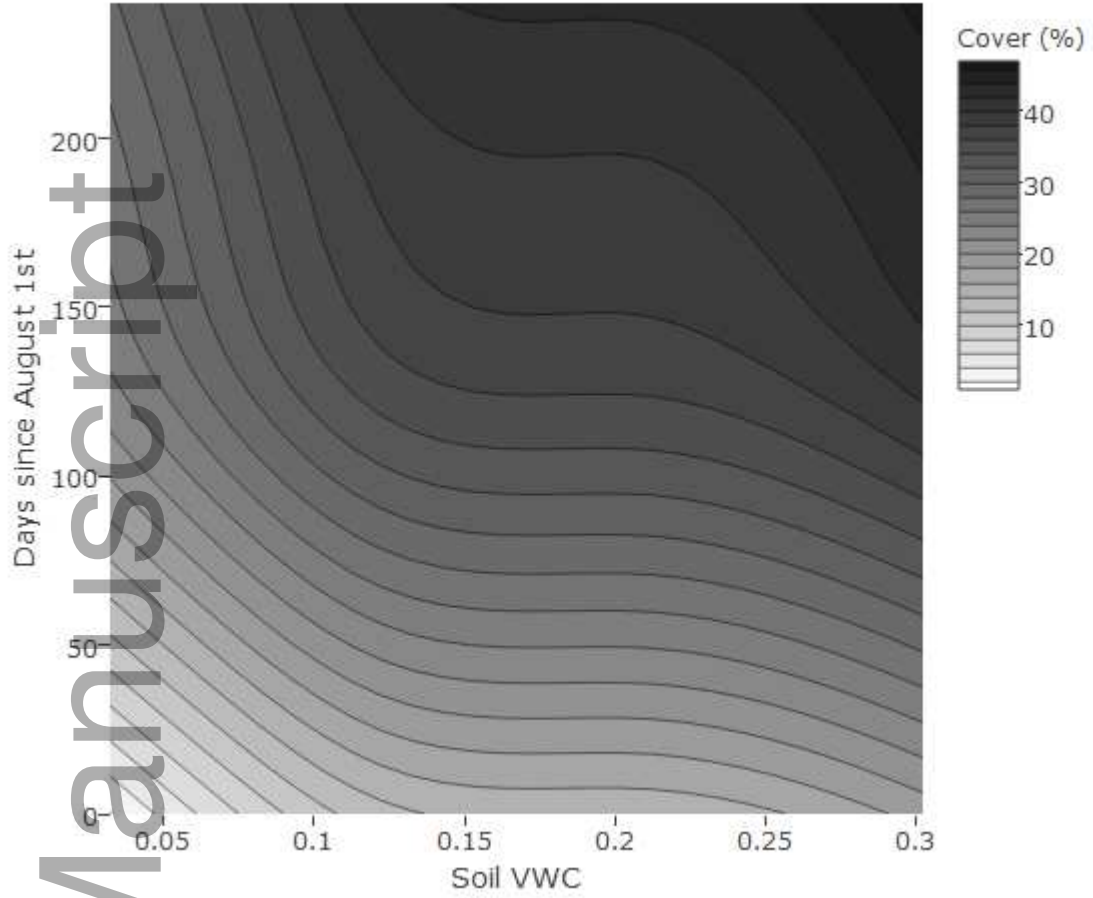
gcb_14038_f3.tiff



gcb_14038_f4.tiff



gcb_14038_f5.tiff



gcb_14038_f6.png